Methods xxx (xxxx) xxx

Contents lists available at ScienceDirect

Methods

journal homepage: www.elsevier.com/locate/ymeth

Mapping circular RNA structures in living cells by SHAPE-MaP

Si-Kun Guo [a,1], Fang Nan [b,1], Chu-Xiao Liu [a], Li Yang [b,c], Ling-Ling Chen [a,c,d,*]

[a] State Key Laboratory of Molecular Biology, Shanghai Key Laboratory of Molecular Andrology, CAS Center for Excellence in Molecular Cell Science, Shanghai Institute of Biochemistry and Cell Biology, University of Chinese Academy of Sciences, Chinese Academy of Sciences, 320 Yueyang Road, Shanghai 200031, China
[b] CAS Key Laboratory of Computational Biology, Shanghai Institute of Nutrition and Health, University of Chinese Academy of Sciences, Chinese Academy of Sciences, 320 Yueyang Road, Shanghai 200031, China
[c] School of Life Science and Technology, ShanghaiTech University, 100 Haike Road, Shanghai 201210, China
[d] School of Life Science, Hangzhou Institute for Advanced Study, University of Chinese Academy of Sciences, Hangzhou 310024, China

ARTICLE INFO

Keywords:
Circular RNA
Secondary structure
Living cell
SHAPE-MaP

ABSTRACT

Circular RNAs are produced from back-splicing of exons of precursor mRNAs (pre-mRNAs). The sequences of exons in circular RNAs are identical to their linear cognate mRNAs, but the circular format may confer constraints on their folding and conformation, leading to potentially different functions from their linear RNA cognates. Here, we describe experimental and computational steps that optimize the selective 2'-hydroxyl acylation analyzed by primer extension and mutational profiling (SHAPE-MaP) to probe circular RNA secondary structure at single-nucleotide resolution in living cells.

1. Introduction

Circular RNAs are produced from pre-mRNAs back-splicing of exons. They have the same sequences, but presumably different structures from their cognate linear RNAs due to the covalently closed circular conformations [1,2]. As a consequence, circular RNAs may have unique features and functions compared with linear cognate mRNAs [2,3]. For example, many circular RNAs tend to form 16–26 bp imperfect double-stranded (ds) duplexes and act as endogenous inhibitors for the dsRNA activated protein kinase PKR during innate immune responses [4]. Beside acting as a group, individual circular RNAs can act differently from cognate linear RNAs by folding into distinct structures. *circANRIL* (circular antisense non-coding RNA in the *INK4* locus) is transcribed from a locus related to atherosclerotic cardiovascular disease on chromosome 9p21. This circular RNA forms a stem loop that binds pescadillo homologue 1 (PES1), an essential 60S pre-ribosomal assembly factor, conferring atheroprotection by controlling ribosomal RNA maturation and modulating atherogenesis [5]. In addition, some highly structured circular RNAs are recognized by the RNA-binding protein UPF1, and subject to degradation by associating with G3BP1 [6]. These emerging studies highlight the importance of understanding structural features of circular RNAs that indispensably link with their life cycles and biological functions.

Based on the integrated computational, biochemical and biophysical methods, systematic structure studies on long non-coding RNA (lncRNA) reveal its complex molecular architecture to dictate understanding of its function [7]. However, because of their covalently closed conformations, predictions of circular RNA structures cannot be simply based on computation using RNA fold algorithm developed in a sequence-dependent manner [4]. Two different principles are developed for probing linear RNA secondary structures: RNase digestion and chemical modification. For the RNase digestion-based methods, RNase S1 or RNase V1, cleaves single- or double- stranded RNA regions, respectively, and can be used to discriminate RNA folding status [8]. Further combination with deep sequencing, comprehensive enzymatic footprinting can be provided by showing RNA secondary structural information for thousands of RNAs at once [9]. For chemical probing methods, dimethylsulfate (DMS) [10], 1-methyl-7-nitroisatoic anhydride (1M7) [11] and 2-methylnicotinic acid imidazolide (NAI) [12] are the widely used chemical molecules. Modification of different bases in an RNA of interest followed by reverse transcription generates cDNA truncations or mutations, reflected by sequencing gel or deep sequencing [13,14].

Among all chemicals, DMS prefers to modify adenosine and cytosine on the Watson-Crick face, and guanosine on the N7 position on the

* Corresponding author at: State Key Laboratory of Molecular Biology, Shanghai Key Laboratory of Molecular Andrology, CAS Center for Excellence in Molecular Cell Science, Shanghai Institute of Biochemistry and Cell Biology, University of Chinese Academy of Sciences, Chinese Academy of Sciences, 320 Yueyang Road, Shanghai 200031, China.
E-mail address: linglingchen@sibcb.ac.cn (L.-L. Chen).
[1] These authors contributed equally.

https://doi.org/10.1016/j.ymeth.2021.01.011
Received 22 November 2020; Received in revised form 21 January 2021; Accepted 29 January 2021
Available online 9 February 2021

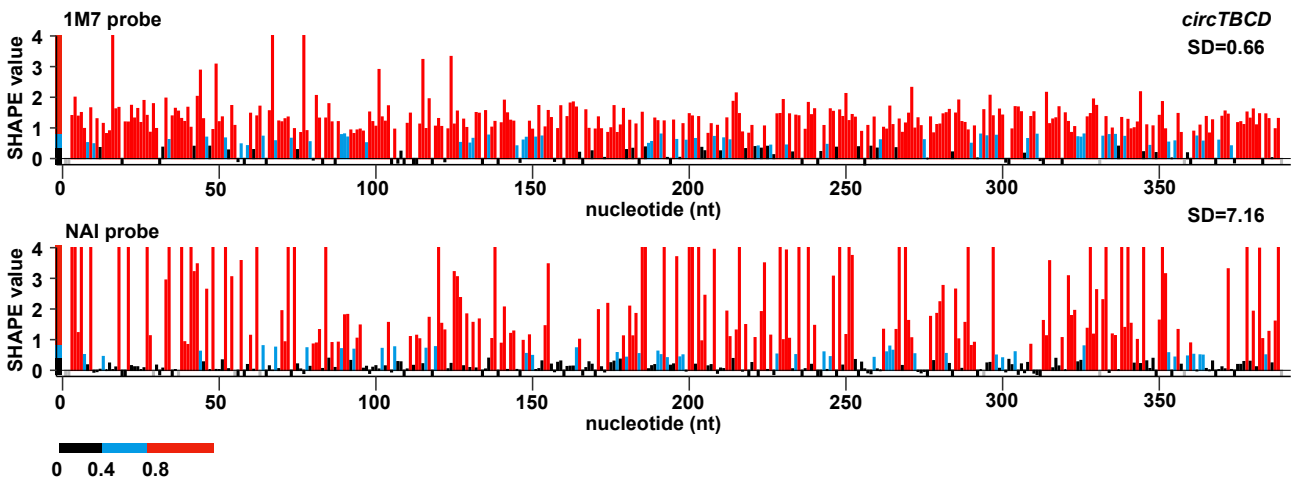

Fig. 1. SHAPE-MaP reactivity profiles of *circTBCD* probed by distinct SHAPE reagents (1M7, top panel; NAI, bottom panel) reveal that NAI performs better for circular RNAs. SHAPE reactivity is calculated by [(Modified$_{MutR}$ – Untreated$_{MutR}$)/Denatured$_{MutR}$] and normalized by a model-free box-plot approach. Reactivities below 0.4 are shown in black, reactivities between 0.4 and 0.8 are shown in blue and reactivities above 0.80 are shown in red. The standard deviation (SD) of SHAPE reactivities is calculated to indicate capabilities of different methods in separating single- or double- stranded regions. SD is the average of the squared distances from SHAPE reactivity of each nucleotide to the mean. (For interpretation of the references to color in this figure legend, the reader is referred to the web version of this article.)

single-stranded RNA [15]. Unlike the base bias of DMS, 1M7 and NAI literarily modify all types of nucleotides [13] and are utilized in multiple *in vitro* SHAPE technologies. However, 1M7 and NAI treatments in cells may lead to different efficiencies of RNA secondary structure analysis [16]. In our hand, NAI showed better reactivities than 1M7 in PA1 cells for the secondary structural probing of circular RNAs, such as *circTBCD* [3], when combined with deep sequencing (Fig. 1). The standard deviation (SD) of *circTBCD* SHAPE reactivities modified by NAI (SD = 7.16) is greater than that by 1M7 (SD = 0.66) (Fig. 1), suggesting that NAI has a better performance in distinguishing single-stranded and double-stranded regions. This result is consistent with a previous report on NAI treatment followed by denaturing gel electrophoresis of mouse 5S rRNA [16].

In addition to different SHAPE reagents, two SHAPE assays, icSHAPE (*in vivo* click selective 2'-hydroxyl acylation and profiling experiment) [17] and SHAPE-MaP [18] have been developed to measure RNA secondary structures in living cells with deep-sequencing. While icSHAPE detects signals on cDNA truncations [15], SHAPE-MaP reads cDNA mutations [16]. In icSHAPE, RNAs are modified in cells by NAI-N3 to include a biotin moiety followed by purification with streptavidin-conjugated beads. The SHAPE reagent adduct blocks reverse transcription elongation at the NAI-N3-modified base to generate a library with corresponding cDNA truncations [17]. For SHAPE-MaP, modified nucleotides are read as mismatches during reverse transcription by deep-sequencing, and SHAPE-modified nucleotides are calculated by SHAPE reactivity [18]. Given the identical sequences of circular and linear cognate RNAs except the back-splice site (Fig. 2A), cDNA mutations provide information in distinguishing circular RNAs from cognate linear RNAs, not cDNA truncations.

In this chapter, we describe an integrated protocol for the analysis of circular RNA secondary structure in cells (Figs. 2 and 4). According to our experience (Fig. 1), we recommend to use NAI as the SHAPE reagent to profile mutant nucleotides for circular RNA secondary structures in cells. In addition to obtaining circSHAPE-MaP signals, the paired linear RNA and 5S rRNA should be used as controls in these assays (Fig. 2). Together, this protocol includes experimental settings for NAI probing and primer designs for circular, cognate linear and 5S RNAs (Figs. 2 and 3A), as well as a computational pipeline specific for circular RNA secondary structural assembly based on deep sequencing results (Fig. 4). Finally, a successful SHAPE-MaP experiment of a circular RNA requires two control reactions in parallel: a non-reagent (DMSO) treatment and a denaturing control (DC) treatment.

There are different requirements to probe circular RNAs and their linear cognates. Firstly, there is no limitation on exon size or sequence length for linear RNAs, because multiple pairs of primers can be designed and amplified to cover the full length of linear RNAs. In contrast, circular RNAs that are appropriate for circSHAPE-MaP analysis often contain lengths no more than 450 nt for a full coverage of structure detection, because the PCR product must span the back-splice junction (BSJ) site to ensure the mutation information is produced from circular RNAs rather than linear RNAs. Consequently, it is critical to design primer pairs that can discriminate circular RNAs from their linear RNA counterparts (Fig. 3A), for details, see Section 3.2, Step 13. Additionally, the circSHAPE-MaP analysis pipeline, CIRCshapemapper, relies on the standard linearSHAPE-MaP pipeline ShapeMapper (v2.1.3) [19] and has been optimized for structure mapping of circular RNAs no more than 450 nt in length. Details of CIRCshapemapper are described in Section 4.

The most common failure of a circSHAPE-MaP experiment is an insufficient circSHAPE-MaP cDNA library which does not produce high-confidence SHAPE reactivity profiles; consequently, the lack of accuracy in structural modeling. We therefore suggest to select circular RNAs on the basis of their abundance, as well as the lack of alternative circularization events of the same exon(s). Ideally, the cognate mRNAs selected for comparison with circular RNAs should display a comparable expression level. Finally, we also recommend to examine sensitivity and specificity of circSHAPE-MaP primers using total RNAs prior to constructing cDNA libraries.

2. Materials

All solutions are prepared from analytical grade chemicals with RNase-free water (TIANGEN, catalog number RT121) or DEPC-treated water (Sangon Biotech, catalog number B501005). Sterilized reagents are aliquoted and stored at 4 °C for immediate usage or at −20 °C for long term storage. As for RNase-free micro centrifuges, 1.5 ml tubes are purchased from Crystalgen (catalog number L-2507), 15 ml centrifuge tubes are from Nest (catalog number 601052) and 50 ml tubes are from Corning (catalog number 430829), respectively.

Equipments required for agarose gel electrophoresis and thermal-cycler are from BIO-RAD (catalog number 165-8001 and T100, respectively). Record gel image by Gel Image System (Tanon, catalog number 3500R) and measure the concentration of nucleotides with Nanodrop

Fig. 2. Schematic of SHAPE modification, reverse transcription reactions, library preparation and construction. A. NAI treatment to probe RNA structures in cells. "*" indicates that a non-reagent treatment (DMSO) and a denaturing control (DC) performed with the NAI treatment in SHAPE-MaP experiments, not shown in the figure. Materials and methods are listed in Section 2.1 and 3.1, respectively. B. Recode NAI modified nucleotides by incorporating NAI-induced mutations to cDNAs by reverse transcriptase. Primer-design principles are listed in Step 13, Section 3.2. C. Nested PCR is used to generate a sufficient amount of sequencing library of each condition in Section 3.3. D. Purification of nested PCR products of individual pairs of circular RNA, cognate linear RNA and 5S rRNA, followed by the library construction for deep-sequencing. The 5S rRNA is an internal control of both circSHAPE-MaP and linearSHAPE-MaP in cells.

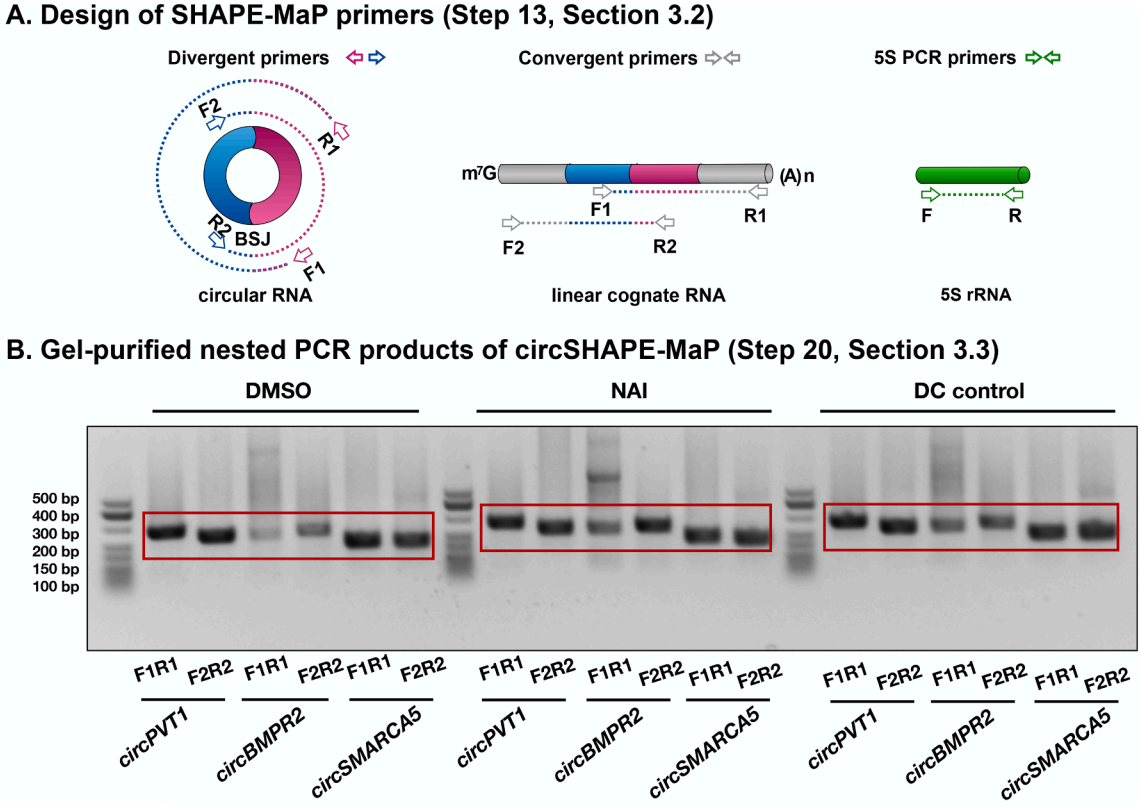

Fig. 3. Primer design principles and gel-purified nested PCR products of circSHAPE-MaP reactions. A. Design of specific primer sets for circular RNA, cognate linear RNA and 5S rRNA. Two pairs of divergent primers spanning the BSJ site of each target circular RNA (150–450 nt in length) are shown to profile the complete secondary structural information [4]. The cognate linear mRNA and 5S rRNA are used as controls with indicated primer sets, see the Step 13 in Section 3.2. B. Gel-purified nested PCR products subjected to deep-sequencing of circSHAPE-MaP. Representative nested PCR products of *circPVT1*, *circBMPR2* and *circSMARCA5* in each experiment setting are shown.

2000.

2.1. SHAPE modification in cells

1. Dulbecco's phosphate-buffered saline (DPBS): GIBCO, catalog number 14190-135.
2. 2-methylnicotinic acid imidazolide (NAI): Millipore, catalog number 03-310.
3. Dimethyl sulfoxide (DMSO): Sigma, catalog number D2650-100ML.
4. TRIZOL Reagent: Invitrogen, catalog number 15596-018.
5. Chloroform: Sigma-Aldrich, catalog number 288306.
6. 75% (v/v) ethanol: dilute 60 ml absolute ethanol with 20 ml DEPC-treated water. Mix well and store at −20 °C.

2.2. SHAPE-MaP reverse transcription

1. DNase: Thermo Fisher, catalog number AM2238.
2. Phenol-chloroform-isoamyl alcohol (25:24:1, v/v): Life Technologies, catalog number 15593-031.
3. 4 M LiCl: weigh 3.3912 g LiCl (Sigma-Aldrich, catalog number L9650-500G) and transfer to a 15 ml RNase-free centrifuge tube, add DEPC-treated water to 10 ml. Mix thoroughly and filter through a 0.22 μm Millex-GP Syringe Filter Unit (Millipore, catalog number SLGP05010). Split into small aliquots and store at −20 °C for usage.
4. 1 M Tris-HCl, pH = 8: Thermo Fisher, catalog number 15568025.
5. 1 M KCl: weigh 11.1825 g KCl (Sigma-Aldrich, catalog number 60130-1 KG) and transfer to a 50 ml RNase-free centrifuge tube, and bring the volume to 50 ml by adding DEPC-treated water. Mix thoroughly and filter through a 0.22 μm Syringe Filter Unit. Store at 4 °C.
6. 1 M DTT (1, 4-Dithioerythritol): weigh 7.7125 g DTT (Merck, catalog number 0281-100G) and transfer to a 50 ml RNase-free centrifuge tube, add DEPC-treated water to 50 ml. Mix thoroughly and filter through a 0.22 μm Millex-GP Syringe Filter Unit. Store at −20 °C for long-term usage.
7. 10 mM dNTPs: TAKARA, catalog number 4019.
8. 1 M HEPES, pH = 8: weigh 11.92 g HEPES (Sigma-Aldrich, catalog number H3375-500G), transfer to a beaker with 50 ml DEPC-treated water, adjust pH to 8.0 with 10 M NaOH. Filter through a 0.22 μm Syringe Filter Unit, and store at 4 °C.
9. 0.5 M EDTA, pH = 8.0: Invitrogen, catalog number 15575020.
10. Formamide: Sigma-Aldrich , catalog number F9037-100ML.
11. RNasin: Promega, catalog number N2515.
12. Superscript II reverse transcriptase: I nvitrogen , catalog number 18064071.

2.3. Library preparation

1. PrimeSTAR HS DNA polymerase: TAKARA,catalog number DR010B.
2. Agarose: ABCONE , catalog number A88490-100G.
3. Gel e xtraction kit: StarPrep, catalog number D205-01

3. Methods

3.1. SHAPE modification in cells

1. Seed three plates of cells with a density of approximately 5x10^6 cells per plate, see Note 1.

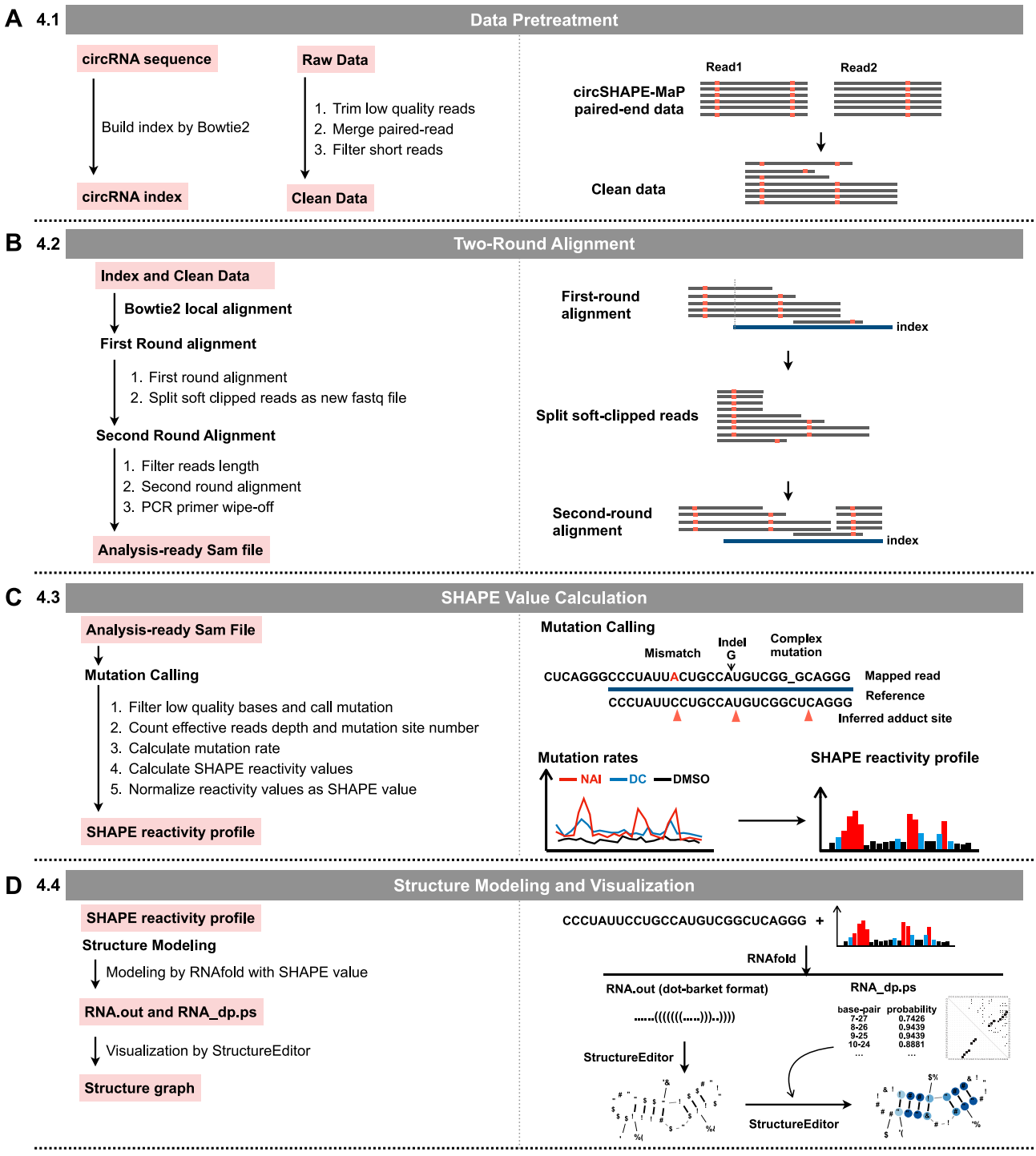

Fig. 4. The pipeline of CIRCshapemapper for circSHAPE-MaP analysis. The detail of each step is listed in Section 4.

2. After washing with DPBS twice, one plate of cells is treated with NAI (2 M dissolved in DMSO) to arrive the final concentration at 200 mM in 1 ml fresh cell culture medium for incubation of 10 min at 37 °C, another one is treated with DMSO in the same volume as the NAI treatment in the same procedure, and the third one is maintained with DPBS for DC reaction (Step 9–11).
3. Add 1 ml DPBS to each plate to wash and repeat once.
4. Treat all three plates of cells with 1 ml Trizol reagent and 200 µl chloroform to isolate RNAs according to the manufacturer's protocol as described [20,21]. Pellet RNAs at 14,000 rpm for 20 min at 4 °C and remove the supernatant into a new tube.
5. Pellet RNAs from cells of three plates using 750 µl prechilled 75% (v/v) ethanol at 14,000 rpm for 5 min at 4 °C twice and air-dry it till the pellets of RNAs are getting clear. Resuspend RNAs in 100 µl RNase-free water. Measure the concentration of RNA samples from three plates. Usually, 50–70 µg total RNAs are collected per plate of cells. For long-term storage of total RNAs, see Note 2.

3.2. SHAPE-MaP reverse transcription

6. Set up DNase treatment reaction as follows:

Reagent	Volume (total is 50 μl)
5 × DNase buffer	10 μl
Total RNAs	10 μg or 15 μg
DNase	1 μl
RNase-free water	~39 μl

For NAI treatment and DMSO treatment, add 10 μg total RNAs to each reaction, as for DC reaction, 15 μg RNAs are used for DNase treatment. Incubate the reaction at 37 °C for 30 min in incubator.

7. After the DNase treatment, add 150 μl RNase-free water to each three tube (NAI treatment, DMSO treatment or DC reaction), to bring the volume to 200 μl.
8. Extract RNAs with 200 μl Phenol-chloroform-isoamyl alcohol (25:24:1, v/v). Transfer ~185 μl supernatant to a clean tube. Add 18.5 μl 4 M LiCl (0.1 times of the 185 μl supernatant) and 555 μl ethanol (3 times of the 185 μl supernatant). Pellet RNAs at 14,000 rpm for 15 min at 4 °C, then wash pellets twice with 75% (v/v) ethanol. Dry and resuspend RNAs in 10 μl RNase-free water.
9. Prepare 10 × DC buffer in 1 ml as follows: 500 mM HEPES (pH = 8) with 40 mM EDTA.
10. Transfer 9 μl RNAs from sample of DC treatment (from Step 8) to a clean tube, add 15 μl 100% formamide and 2.6 μl 10 × DC buffer. Incubate at 95 °C for 1 min. Add 3 μl 2 M NAI to above solution. Incubate at 95 °C for 1 min and then bring the volume to 100 μl with RNase-free water.
11. Extract NAI-probed RNAs on DC treatment with 100 μl phenol–chloroform–isoamyl alcohol, and transfer supernatant to a clean tube. Pellet RNAs with 300 μl ethanol, 2 μl glycogen and 10 μl 4 M LiCl. Wash pellets with 750 μl of 75% (v/v) ethanol at 14,000 rpm for 15 min at 4 °C and air-dry, then resuspend it in 10 μl RNase-free water.
12. Prepare 5 × MaP pre-buffer as follows:

Stock solution concentration	Volume (total is 100 μl)	Working concentration
1 M Tris-HCl, pH = 8	25 μl	250 mM
1 M KCl	12.5 μl	125 mM KCl
1 M DTT	5 μl	50 mM DTT
10 mM dNTPs	25 μl	2.5 mM dNTPs
RNase-free water	32.5 μl	

13. Design RT-PCR primer:

Human 5S rRNA is detected as an internal control in both circSHAPE-MaP and linearSHAPE-MaP assays.

For circSHAPE-MaP, two sets of divergent primers crossing the BSJ site are designed. Circular RNAs with 150–450 nt in length are targeted by two sets of primers to cover sequences for structural detection.

circSHAPE-MaP primers are designed based on three criteria (Fig. 3A):

A. NAI probing in cells gives rise to consistent and reliable signals for SHAPE-MaP assays with 300 bp long tiling PCR products for circular RNAs.

B. Two sets of divergent primers of circSHAPE-MaP should be designed to cross the BSJ site in order to discriminate circular RNAs from their cognate mRNAs.

C. A greater than 50 bp overlapping region should be covered by these two pairs of divergent primers.

For linearSHAPE-MaP, design multiple sets of convergent primers to amplify the signal in circular RNA-forming exons and their flaked non-circular RNA-forming exons (Fig. 3A). In such a setting, we recommend the size of around 300 bp length of non-circular RNA-forming exons on each side of circular RNA-forming exons to be amplified in linearSHAPE-MaP.

14. Set up reverse transcription reactions as follows (Fig. 2B):

Add 3 μl RNAs of each sample (RNA sample of NAI or DMSO treatment is from Step 8 and DC treatment is from Step 11) with 7.5 μl reverse primer mix (from Step13, 2 pmol for each primer used, no more than 10 primers for each reaction is recommended), incubate samples at 65 °C for 5 min and chill on ice for 2 min.

15. Prepare 2.5 × MaP buffer by mixing 50 μl 5 × MaP pre-buffer with 50 μl 30 mM $MnCl_2$.
16. Add 8 μl 2.5 × MaP buffer, 0.5 μl RNasin and 1 μl Superscript II reverse transcriptase to the solution of Step14 (see Note 3). Incubate at 42 °C for 3 h and heat the reactions at 70 °C for 15 min to inactivate Superscript II reverse transcriptase. The reverse transcription products are ready for use or kept at −20 °C for weeks.

3.3. Library preparation and sequencing

Nested PCR strategy (Fig. 2C) is used. Nested PCR is intended to reduce non-specific products, thus involving two sets of primer in two sequential amplification reactions. The first pair of PCR primers amplifies a fragment similar to a standard PCR. Additionally, the product of the first amplification reaction is used as the template for the secondary PCR reaction, which is primed by oligonucleotides that are placed internal to the first primer pair [22]. Set up the first PCR reaction as follows:

Reagent	Volume (total is 50 μl)
5 × buffer	10 μl
10 mM dNTPs	4 μl
20 μM forward primer	1 μl
20 μM reverse primer	1 μl
cDNAs from Step 16	2 μl
PrimeSTAR HS DNA polymerase	0.5 μl
RNase-free water	31.5 μl

18. Set up first PCR cycles as follows:

98 °C	2 min
98 °C	10 s
55 °C	15 s 25 ~ 30 cycles
72 °C	30 ~ 60 s20 μM forward primer
72 °C	5 min

19. Set up second PCR reaction with nested primers and PCR products from Step 18 similarly as the first PCR reaction. Resolve PCR product on 1.5% agarose at 120 v for 20 min and record gel image by gel image system.
20. Purify cDNAs from gel slice. These PCR products from the RNAs with different treatment (DMSO, NAI or DC treatment) are similar in size, as shown in Fig. 3B. Cut gel slide in red square and purify it as a mixture according to the manufacturer's protocol.
21. Measure sample concentration for subsequent deep sequencing.

4. Deep sequencing and analysis

SHAPE-MaP libraries are prepared from 1 ng of gel-purified cDNAs (circular RNAs, cognate linear RNAs or 5S RNAs) from Step 21 by using Illumina TruSeq ChIP Sample Prep Kit without ultrasonic disruption step and deep-sequenced to obtain 150 bp paired-end reads. Of an important note, linearSHAPE-MaP and circSHAPE-MaP libraries are prepared separately with different indexes to distinguish reads from linear RNAs and circular RNAs. For cognate linear RNAs and 5S RNA, mutations are

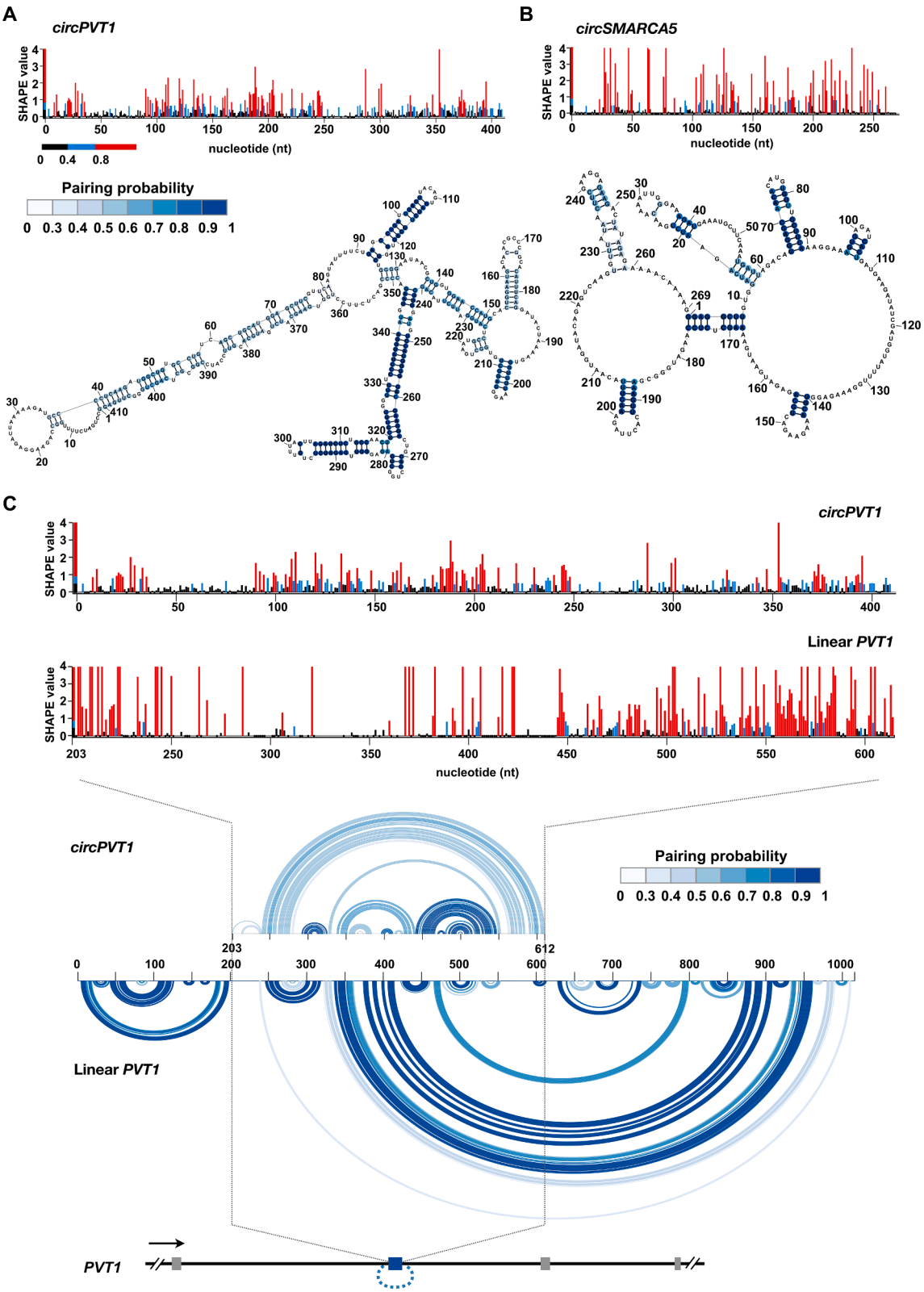

Fig. 5. The SHAPE reactivities (top) and the secondary structure (bottom) of *circPVT1* (A) and *circSMARCA5* (B). A and B. The SHAPE reactivities generated by CIRCshapemapper pipeline are shown. The secondary structure is predicted by RNAfold with SHAPE values. Potential base pairs are shown as color arcs indicting pair probabilities. C. SHAPE reactivities and structure differences of circular and cognate linear *PVT1*. The *PVT1* locus is shown underneath and *circPVT1*-forming exon is indicated in blue. (For interpretation of the references to color in this figure legend, the reader is referred to the web version of this article.)

counted to create SHAPE reactivity profiles using ShapeMapper (v2.1.3) [19]; for circular RNAs, we develop a customized pipeline, CIRCshapemapper [4] (Fig. 4) (https://github.com/YangLab/CIRCshapemapper), to analyze circSHAPE-MaP data and predict secondary structures of circular RNAs. This pipeline is amended according to ShapeMapper (v2.1.3) [19] with default parameters (–target RNA.fa –out folder –nproc 16 –verbose –serial –min-depth 1000 –modified –untreated –denatured) for the secondary structure analysis of circular RNAs. The entire analysis pipeline includes four sections: data pretreatment (Section 4.1; Fig. 4A); the two-round alignment (Section 4.2; Fig. 4B); SHAPE value calculation (Section 4.3; Fig. 4C); circular RNA secondary structure modeling and visualization (Section 4.4; Fig. 4D). Based on experimental results, the two-round alignment (Section 4.2; Fig. 4B) is applied to improve the mapping accuracy for circSHAPE-MaP. Of note, this section is a key step in circSHAPE-MaP analyses. Section 4.3 describes the principles of mutation calling and SHAPE value calculation (Fig. 4C). And Section 4.4 describes the prediction and visualization of secondary structures of circular RNAs with paring probability (Fig. 4D). Details of each part in CIRCshapemapper are listed below.

4.1. Data pretreatment

Before alignment, the indexes of target circular RNAs are built by bowtie2-build of Bowtie2 with RNA sequences in which "U" replaced by "T". Quality control of raw deep sequencing reads is needed before alignment. Briefly, sequencing reads are scanned from left to right and trimmed right nucleotides according to a 5-nt window whose average quality score is less than 20. Reads with 25 nt in length are kept for the subsequent analysis. After that, paired reads with overlapped sequences are merged into single reads and remanent paired reads without overlapping are de-associated as single reads.

4.2. Two-round alignment

After aforementioned pretreatment, two-round alignment is applied to map reads across BSJ of circSHAPE-MaP to improve the accuracy of mapping efficiency. Briefly, pre-processed reads are mapped to the index of target RNA sequences by Bowtie2 (v2.1.0) (–local –sensitive-local –mp 3,1 –rdg 5,1 –rfg 5,1 –dpad 30 –maxins 800 –ignore-quals no-unal). Here, the local alignment mode is applied to get a maximal alignment score via clipping some nucleotides on both ends that are not matched with reference indexes. After that, soft clipped reads are split and combined with the first-round mapped reads into fastq format file for the second-round alignment. Of note, split reads shorter than 25 nt are wiped off before second-round alignment. After this two-round alignment, sequences located at 5' end of reads which are matched with PCR primers are removed and their alignment information in bam file are accordingly modified.

4.3. SHAPE value calculation

To determine mutation sites of each read, alignment information in the bam file of each mapped read is parsed to identify mutated location. Counts of un-mutated or mutated nucleotides at each location are obtained from mapped reads. Of note, counts from nucleotides with low Phred quality score ($\leq$30) at each examined location are excluded. In addition, locations whose minimum read depths are fewer than 1,000 will not be included for the subsequent calculation of mutation ratio (MutR). Finally, SHAPE reactivity is calculated by [($\text{Modified}_{\text{MutR}}$ – $\text{Untreated}_{\text{MutR}}$)/$\text{Denatured}_{\text{MutR}}$] and further normalized to get SHAPE profile for modeling RNA secondary structure. Scripts published in ShapeMapper (v2.1.3) are used for all the analyses.

4.4. Structure modeling and visualization

The circular RNA secondary structure prediction is based on the SHAPE reactivity profile by RNAfold (v2.4.2) in ViennaRNA [23] package with the specific parameters: -p -d2 –circ –shape = SHAPE reactivity profile –shapeMethod = D < RNA.fa. Target RNA sequence in the input RNA.fa file is matched with that of SHAPE reactivity profile. Two output files are obtained: one for pairing probability matrix in an RNA_dp.ps file and the other one for the circular RNA secondary structure in a dot-bracket format (.out) file. The secondary structure of circular RNAs can be visualized by StructureEditor software with the dot-bracket format (.out) file as the input file. By including the pairing probabilities of double-stranded sequences from RNA_dp.ps, a better graph of circular RNA secondary structure can be obtained by StructureEditor. Different secondary structure features, such as double-stranded sequence, hairpin, bulge and internal loop, can be retrieved by further analyzing the structure graph (Fig. 5).

5. Notes

1. For each experimental setting of circSHAPE-MaP, three plates of cells are prepared for NAI modification, DMSO treatment or DC treatment, respectively. We took PA1 cells as an example to map circular RNA structures in this method, however, the same protocol should be applicable to other cultured cell lines.
2. For long-term storage of RNAs subjected with SHAPE treatments, we advise to store such modified RNAs in pre-chilled 75% (v/v) ethanol at −80 °C.
3. Superscript II reverse transcriptase in the working solution is unstable and the operation must be performed immediately in 30 min.

Declaration of Competing Interest

The authors declare that they have no known competing financial interests or personal relationships that could have appeared to influence the work reported in this paper.

Acknowledgments

This work was supported by the National Natural Science Foundation of China (NSFC) (91940303, 31725009, 31821004), the Chinese Academy of Sciences (CAS) (XDB19020104) and the HHMI International Program (55008728) to L.-L.C. L.-L.C. acknowledges the support from the XPLORER PRIZE.

References

[1] X. Li, L.i. Yang, L.-L. Chen, The Biogenesis, Functions, and Challenges of Circular RNAs, Mol. Cell 71 (3) (2018) 428–442.
[2] L.-L. Chen, The expanding regulatory mechanisms and cellular functions of circular RNAs, Nat. Rev. Mol. Cell Biol. 21 (8) (2020) 475–490.
[3] M.-S. Xiao, Y. Ai, J.E. Wilusz, Biogenesis and Functions of Circular RNAs Come into Focus, Trends Cell Biol. 30 (3) (2020) 226–240.
[4] C.-X. Liu, X. Li, F. Nan, S. Jiang, X. Gao, S.-K. Guo, W. Xue, Y. Cui, K. Dong, H. Ding, B.o. Qu, Z. Zhou, N. Shen, L.i. Yang, L.-L. Chen, Structure and Degradation of Circular RNAs Regulate PKR Activation in Innate Immunity, Cell 177 (4) (2019) 865–880.e21.
[5] L.M. Holdt, A. Stahringer, K. Sass, G. Pichler, N.A. Kulak, W. Wilfert, A. Kohlmaier, A. Herbst, B.H. Northoff, A. Nicolaou, G. Gabel, F. Beutner, M. Scholz, J. Thiery, K. Musunuru, K. Krohn, M. Mann, D. Teupser, Circular non-coding RNA ANRIL modulates ribosomal RNA maturation and atherosclerosis in humans, Nat. Commun. 7 (2016) 12429.
[6] J.W. Fischer, V.F. Busa, Y. Shao, A.K.L. Leung, Structure-Mediated RNA Decay by UPF1 and G3BP1, Mol. Cell 78 (1) (2020) 70–84.e6.
[7] I. Chillon, M. Marcia, The molecular structure of long non-coding RNAs: emerging patterns and functional implications, Crit. Rev. Biochem. Mol. Biol. 55 (6) (2020) 662–690.
[8] P.E. Auron, L.D. Weber, A. Rich, Comparison of transfer ribonucleic acid structures using cobra venom and S1 endonucleases, Biochemistry 21 (19) (1982) 4700–4706.
[9] Y. Wan, K. Qu, Z. Ouyang, H.Y. Chang, Genome-wide mapping of RNA structure using nuclease digestion and high-throughput sequencing, Nat. Protoc. 8 (5) (2013) 849–869.
[10] A.R.W. Schroder, T. Baumstark, D. Riesner, Chemical mapping of co-existing RNA structures, Nucleic Acids Res. 26 (14) (1998) 3449–3450.

[11] S.A. Mortimer, K.M. Weeks, A fast-acting reagent for accurate analysis of RNA secondary and tertiary structure by SHAPE chemistry, J. Am. Chem. Soc. 129 (14) (2007) 4144–4145.
[12] R.C. Spitale, P. Crisalli, R.A. Flynn, E.A. Torre, E.T. Kool, H.Y. Chang, RNA SHAPE analysis in living cells, Nat. Chem. Biol. 9 (1) (2013) 18–20.
[13] K.M. Weeks, D.M. Mauger, Exploring RNA structural codes with SHAPE chemistry, Acc. Chem. Res. 44 (12) (2011) 1280–1291.
[14] D.M. Mauger, M. Golden, D. Yamane, S. Williford, S.M. Lemon, D.P. Martin, K. M. Weeks, Functionally conserved architecture of hepatitis C virus RNA genomes, Proc. Natl. Acad. Sci. U.S.A. 112 (12) (2015) 3692–3697.
[15] D.A. Peattie, W. Gilbert, Chemical probes for higher-order structure in RNA, Proc Natl Acad Sci U S A 77 (8) (1980) 4679–4682.
[16] B. Lee, R.A. Flynn, A. Kadina, J.K. Guo, E.T. Kool, H.Y. Chang, Comparison of SHAPE reagents for mapping RNA structures inside living cells, RNA 23 (2) (2017) 169–174.
[17] R.A. Flynn, Q.C. Zhang, R.C. Spitale, B. Lee, M.R. Mumbach, H.Y. Chang, Transcriptome-wide interrogation of RNA secondary structure in living cells with icSHAPE, Nat. Protoc. 11 (2) (2016) 273–290.
[18] M.J. Smola, G.M. Rice, S. Busan, N.A. Siegfried, K.M. Weeks, Selective 2'-hydroxyl acylation analyzed by primer extension and mutational profiling (SHAPE-MaP) for direct, versatile and accurate RNA structure analysis, Nat. Protoc. 10 (11) (2015) 1643–1669.
[19] S. Busan, K.M. Weeks, Accurate detection of chemical modifications in RNA by mutational profiling (MaP) with ShapeMapper 2, RNA 24 (2) (2018) 143–148.
[20] Q.F. Yin, L.L. Chen, L. Yang, Fractionation of non-polyadenylated and ribosomal-free RNAs from mammalian cells, Methods Mol. Biol. 1206 (2015) 69–80.
[21] Y. Zhang, L. Yang, L.L. Chen, Characterization of Circular RNAs, Methods Mol. Biol. 1402 (2016) 215–227.
[22] M.R. Green, J. Sambrook, Nested Polymerase Chain Reaction (PCR), Cold Spring Harb. Protoc. 2019(2) (2019).
[23] R. Lorenz, S.H. Bernhart, C. Honer Zu Siederdissen, H. Tafer, C. Flamm, P.F. Stadler, I.L. Hofacker, ViennaRNA Package 2.0, Algorithms Mol. Biol. 6 (2011) 26.